How a rotating magnetic field causes ferrofluid to rotate

Mark I. Shliomis*

Department of Mechanical Engineering, Ben-Gurion University of the Negev, Beer-Sheva 84105, Israel

(Received 11 September 2020; accepted 29 March 2021; published 19 April 2021)

The article explores the various mechanisms by which a rotating magnetic field causes to rotate a magnetic fluid contained in a cylinder (the so-called spin-up of ferrofluids). It is shown first that the generally accepted theory of spin diffusion cannot explain this phenomenon due to the extremely low spin viscosity η': Our calculations give $\eta' \sim 10^{-14}$ g cm/s which is 11 orders of magnitude less than the most optimistic estimates. Then we develop a theory linking the rotation of a free surface layer to the shape of the meniscus. The latter, equally as the strength and frequency of the rotating field, determines both the direction and the magnitude of the fluid velocity. However, the magnetic torque created on the curved surface of the liquid captures only a thin subsurface layer and does not cause rotation in the volume. As for the volumetric flow, we associate it with the release of heat in microvortices that arise around rotating magnetic particles. In a vertical cylinder, such heating forms a parabolic temperature profile, which makes the magnetization of the fluid spatially inhomogeneous. As shown, this is sufficient to induce an observable bulk flow of the ferrofluid. The influence of natural convection on this spin-up flow is also investigated. In conclusion, it is shown that the stress tensor of a magnetic fluid can always be brought to a symmetric form.

DOI: 10.1103/PhysRevFluids.6.043701

I. INTRODUCTION

Ferrofluids are colloidal suspensions of magnetic particles with a diameter of 10–20 nm. The close interweaving of the magnetic and rotational degrees of freedom of particles gives rise to a number of interesting hydrodynamic phenomena. They occur in a time-varying magnetic field **H** where the fluid magnetization **M** due to its finite relaxation time turns out to be noncollinear to **H**. As a consequence, the magnetic torque $\mathbf{M} \times \mathbf{H}$ takes on nonzero values. Oscillating magnetic fields cause impressive effects in moving fluids, such as "negative viscosity" [1–3] and vortical-magnetic resonance [4,5]. A rotating magnetic field can induce rotation in a stationary fluid. This *spin-up* phenomenon has a 50-yr history; it was first studied by Moskowitz and Rosensweig [6] experimentally and by Zaitsev and Shliomis [7] theoretically.

Spin-up occurs when a liquid placed in a vertical cylinder is exposed to a horizontal uniform magnetic field rotating around the axis of the cylinder in its cross section. When the field rotates, magnetic particles become centers of microscopic vortices (*microeddies*). The hydrodynamics of fluids with such *internal rotation* (of "molecules with spin" in Frenkel's terminology [8]) was developed by Condiff and Dahler [9] and Shliomis [10] even before [6]. The equation of particles rotation obtained in Ref. [10] formed the basis for "the theoretical discovery of purely vortex flows in the work of Zaitsev and Shliomis, who presented this concept in an attempt to rationalize the Moskowitz and Rosensweig swirl-flow experiment" (Brenner [11]).

*shliomis@bgu.ac.il, mshliomis@gmail.com

According to this concept, known as spin-diffusion theory, the spin of particles (latent rotation) can be converted into angular momentum of macroscopic (hydrodynamic) flow. The decisive role in this transformation is played by the kinetic coefficient η' called spin viscosity. Its value is not known: "We are left with a discrepancy between estimates of the spin viscosity spanning eight to ten orders of magnitude," wrote Finlayson in his in-depth review [12]. This leads to discrepancies between theoretical predictions and experimental results on the spin-up flow velocity. Even the direction of fluid rotation—the same as the rotating field or the opposite—is still debated. Shortly after the work [6], Brown and Horsnell had reported [13] under the heading "The wrong way round" about the field and fluid corotation at weak applied fields and their counter-rotation when the field strength increased. Similar conclusions were obtained by Kagan *et al.* [14]. Later Rosensweig *et al.* found a connection between the direction of rotation of the fluid and the shape of its free surface: The fluid rotated in the same direction as the field when the meniscus was concave and opposite to the field when the meniscus was convex [15].

Note that the velocity measurements in Refs. [6,13–15] were carried out on the free surface of the fluid. Measurements in the bulk are complicated due to ferrofluid opacity. Rosenthal *et al.* [16] measured the frictional torque acting on a cylinder, fully filled with a ferrofluid, and made sure that "the torque exists: It does not need a free surface" (indeed, as will be shown, the torque requires neither a free surface nor a flow of ferrofluid). Chaves and co-workers [17,18] and Torres-Diaz *et al.* [19] used the ultrasonic techniques to measure the velocity in the bulk and found that the field and fluid rotate in the same direction—as prescribed by spin-diffusion theory. On the contrary, Lebedev and Pshenichnikov [20] clearly demonstrated the counter-rotation; they estimated the flow rate from the angle of rotation of a wire frame suspended by a flexible thread in the middle of the cylinder.

In the present paper, we have revised the spin-up problem. In Sec. II, we determined the value of the spin viscosity η', which turned out to be 11–12 orders of magnitude less than the highest estimate, $\eta' \simeq 10^{-3}$ g cm/s, performed in Ref. [19]. The reason for this smallness lies in the huge difference between the total moment of inertia of microeddies and the moment of inertia of a macroscopic vortex the size of a cylinder radius. For this reason, the entrainment of a ferrofluid by a rotating magnetic field (if any!) cannot be explained on the basis of the theory of spin diffusion. This inference cannot be better formulated than was performed by Rosensweig *et al.* [15]: "We have not previously encountered a physical system in which so many experimental facts supported a theory yet the theory [of spin diffusion] was inapplicable."

Therefore, in what follows we put $\eta' = 0$ and reconsider the surface coupling mechanism of spin-up phenomenon in Sec. III. Then, in Sec. IV, we investigate the thermal effect associated with the dissipation of the energy of a rotating field in microeddies. The heat generated in them makes the temperature and, as a consequence, the fluid magnetization and the field spatially inhomogeneous. The resulting ponderomotive forces cause the fluid to rotate. This mechanism is quite effective since the heat release increases in proportion to the square of the field rotation frequency, thus, the fluid velocity increases as a cube of this frequency. However, natural convection caused by internal heating limits the temperature rise since when the fluid is stirred, it homogenizes the magnetization, thereby eliminating the very cause of the spin-up effect. Some experimental results are discussed in Sec. V. The problem of the symmetry of the stress tensor plays an important role in the theory of fluids with internal rotation. In Appendix B, we demonstrate how you can always bring the stress tensor of ferrofluids to a symmetric form.

II. SPIN-DIFFUSION THEORY

A. Preliminary estimates

The rotating magnetic field creates microeddies around magnetic particles (see Fig. 1). The typical size of such vortices is approximately equal to the distance between particles. Some part of the *latent* angular momentum of microeddies can transform into a *visible* (i.e., hydrodynamic) form. It is easy to show, however, that this part is negligible.

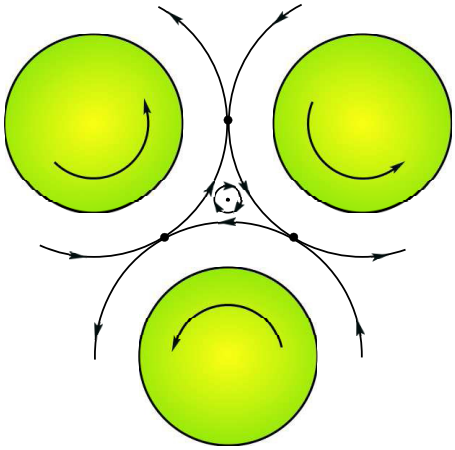

FIG. 1. Rotation of particles in a ferrofluid about their own axes in a rotating magnetic field. Each nanoparticle rotates with the angular velocity $\boldsymbol{\omega}$, however, the macroscopic fluid velocity vanishes by symmetry. The sketch depicts the configuration of streamlines. The circulation caused by the rotation of the particle is precisely compensated by the oppositely directed circulation of its neighbors. Observe the existence of *stagnation points* because of the closure of all streamlines upon themselves.

Let $\boldsymbol{\omega} - \boldsymbol{\Omega}$ be an excess of the angular velocity of particles over half the vorticity, which is the angular velocity of the fluid $\boldsymbol{\Omega} = (\nabla \times \mathbf{v})/2$. The total moment of inertia of microeddies is $I_{\text{mic}} \sim (\mu b^2)N$, where μ and b are the mass and diameter of microeddies, the total number of which in the cylinder is N. The moment of inertia of a liquid cylinder of radius R is $I_{\text{cyl}} \sim (\mu N)R^2$.

In a rotating magnetic field, the total angular momentum is the sum of the internal and hydrodynamic angular momenta $I_{\text{mic}}(\boldsymbol{\omega} - \boldsymbol{\Omega}) + I_{\text{cyl}}\boldsymbol{\Omega}$. After a sudden shutdown of the field, the particle rotation speed $\boldsymbol{\omega}$ immediately decreases to $\boldsymbol{\Omega}$, i.e., latent rotation disappears, becoming visible. This transformation obeys the law of conservation of angular momentum, which in this case has the form

$$I_{\text{mic}}(\boldsymbol{\omega} - \boldsymbol{\Omega}) + I_{\text{cyl}}\boldsymbol{\Omega} = I_{\text{cyl}}\boldsymbol{\Omega}',$$

where $\boldsymbol{\Omega}$ and $\boldsymbol{\Omega}'$ are the angular velocities of the fluid before and after the field is turned off. This equation determines the velocity gain,

$$\delta\boldsymbol{\Omega} = \boldsymbol{\Omega}' - \boldsymbol{\Omega} = \left(\frac{b}{R}\right)^2 (\boldsymbol{\omega} - \boldsymbol{\Omega}).$$

In ferrofluids, b does not exceed 50 nm, whereas $R \sim 1$ cm. Therefore, $(b/R)^2 \sim 10^{-11}$ and the addition of $\delta\boldsymbol{\Omega}$ is vanishingly small.

The smallness of the internal angular momentum is aggravated by difficulties of converting it into translational motion of the fluid. The point is that microeddies disappear due to symmetry upon averaging, such as elementary electric currents of neighboring molecules in Ampere's model of ferromagnetism do that. All streamlines surrounding the particles turn out to be closed on themselves as shown in Fig. 1. Nevertheless, symmetry violations do exist. They are due to the boundary conditions for the spin velocity $\boldsymbol{\omega}$ on the cylinder wall. Thanks to them, the microeddies cease to fully compensate each other, and some of their latent rotation transforms into a hydrodynamic form. Only one key question remains: How large will the macroscopic vortex be?

B. Equations of motion and spin viscosity value

In a uniform rotating magnetic field, equations of ferrofluid motion (1) and particle spin (2) are [7,10]

$$\rho\frac{d\mathbf{u}}{dt} = -\boldsymbol{\nabla} p + \eta\nabla^2\mathbf{u} + \frac{I}{2\tau_s}\boldsymbol{\nabla}\times(\boldsymbol{\omega}-\boldsymbol{\Omega}), \tag{1}$$

$$I\frac{d\boldsymbol{\omega}}{dt} = \mathbf{M}\times\mathbf{H} - \frac{I}{\tau_s}(\boldsymbol{\omega}-\boldsymbol{\Omega}) + \eta'\nabla^2\boldsymbol{\omega}. \tag{2}$$

Here I is the moment of inertia of the particles per unit volume of the ferrofluid (so $\mathbf{S} = I\boldsymbol{\omega}$ is the spin density), τ_s is the spin-relaxation time, and η' is the spin viscosity (the ratio η'/I is the spin-diffusion coefficient). The cross term in these equations, caused by the magnetic torque $\mathbf{M}\times\mathbf{H}$, provides the transformation of the spin of particles $I(\boldsymbol{\omega}-\boldsymbol{\Omega})$ into a hydrodynamic linear momentum. The last term in Eq. (2) plays a critical role in this transformation. If $\eta' = 0$, then in the steay state we arrive—excluding the cross term from (1)—to the equation,

$$\eta\nabla^2\boldsymbol{u} + \tfrac{1}{2}\boldsymbol{\nabla}\times(\mathbf{M}\times\mathbf{H}) = \boldsymbol{\nabla} p. \tag{3}$$

But curl$(\mathbf{M}\times\mathbf{H})$ is zero as $\mathbf{M}$ and $\mathbf{H}$ are spatially uniform, so the fluid velocity is also zero.

After applying the curl operator to Eq. (1), rewrite it and Eq. (2) in the form

$$\underline{\rho\frac{d\boldsymbol{\Omega}}{dt} = \eta\nabla^2\boldsymbol{\Omega}} - \frac{I}{4\tau_s}\nabla^2(\boldsymbol{\omega}-\boldsymbol{\Omega}), \tag{4}$$

$$\underline{I\frac{d\boldsymbol{\omega}}{dt} = \eta'\nabla^2\boldsymbol{\omega}} - \frac{I}{\tau_s}(\boldsymbol{\omega}-\boldsymbol{\Omega}) + \mathbf{M}\times\mathbf{H}. \tag{5}$$

If you turn off the rotating field, both angular velocities $\boldsymbol{\Omega}$ and $\boldsymbol{\omega}$ will decay. This decay occurs in two stages: First, the spin velocity $\boldsymbol{\omega}$ instantly drops to $\boldsymbol{\Omega}$ (see Appendix A for details) after which only the underlined terms remain in Eqs. (4) and (5). Replacing now $\boldsymbol{\omega}$ by $\boldsymbol{\Omega}$ in (5), we come to equations,

$$\rho\frac{d\boldsymbol{\Omega}}{dt} = \eta\nabla^2\boldsymbol{\Omega} \quad \text{and} \quad I\frac{d\boldsymbol{\Omega}}{dt} = \eta'\nabla^2\boldsymbol{\Omega},$$

describing the second stage of relaxation: the decay of a macroscopic vortex in macroscale time $\sim\rho R^2/\eta$. Comparison of these two equations gives the value of spin viscosity,

$$\eta' = \eta I/\rho. \tag{6}$$

Commenting on this result, it is worth noting that this is a rare example when, based on simple physical arguments, it is possible to express the unknown kinetic coefficient (η') in terms of the known (η).

Let us estimate the spin viscosity value. Magnetic particles in a ferrofluid are coated with a surfactant layer to prevent them from coagulating due to their van der Waals and the magnetic dipole attraction. Because of this, the hydrodynamic particle diameter d_h is 2.0–2.5 times larger than the diameter d_m of its magnetic core [21] (see Fig. 2). The moment of inertia of such particles contained in a unit volume of the colloid is

$$I = \frac{1}{10}\hat{\rho}\,\phi d_h^2, \quad \hat{\rho} = \rho_{\text{coat}}\left[1 + \left(\frac{\rho_{\text{mag}}}{\rho_{\text{coat}}} - 1\right)\left(\frac{d_m}{d_h}\right)^5\right]. \tag{7}$$

Here $\phi = (d_h/d_m)^3\phi_m$ is the volume fraction of coated magnetic grains, and $\hat{\rho}$ is their "effective" average density. Because of high power of the ratio d_m/d_h in $\hat{\rho}$, the latter turns out to be close to the density of coating ρ_{coat} and, therefore, differs little from the density ρ of the ferrofluid. Substitution of I from (7) to (6) gives

$$\eta' = \tfrac{1}{10}(\hat{\rho}/\rho)\eta\phi d_h^2. \tag{8}$$

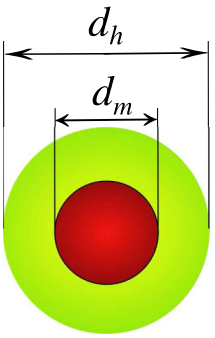

FIG. 2. Ferrofluid particle model: magnetic core of diameter d_m covered with a surfactant layer of the thickness $(d_h - d_m)/2$.

The cobalt-ferrite ferrofluid used by Torres-Diaz *et al.* [19] to study the spin-up effect seems to be most suitable for this purpose. The domain magnetization $M_d = 425$ G of $CoFe_2O_4$ is slightly lower than that of the popular magnetite, but the high magnetic anisotropy of Co-ferrite prevents spontaneous reorientation of the magnetic moments of particles inside them (the Néel fluctuation mechanism is "frozen" [22]). For a water-based ferrofluid designated in Ref. [19] as WBF-2, where $d_m = 17$, $d_h = 39$ nm, $\eta_0 = 1.02$ cP, in the case of magnetic volume fraction $\phi_m = 2\%$ [and, hence, hydrodynamic fraction $\phi = (39/17)^3\phi_m = 24\%$] the saturation magnetization $M_{\rm sat} = \phi_m M_d = 8.5$ G and the Langevin parameter $\alpha = mH/kT = 1$ in the field $H = 37.5$ Oe.

The viscosity of ferrofluids is quite satisfactory described by the relations,

$$\eta = \eta_0\left(\frac{2-\phi}{2-3\phi}\right)^E, \quad E = 2.5 + 1.5\Gamma(\alpha), \quad \Gamma(\alpha) = \frac{\alpha\mathcal{L}(\alpha)}{2+\alpha\mathcal{L}(\alpha)} = \frac{\alpha - \tanh\,\alpha}{\alpha + \tanh\,\alpha}, \tag{9}$$

which in the case of dilute magnetic colloids turns into the formula $\eta = \eta_0(1 + E\phi)$ given in Ref. [23]. As a result, for the indicated ferrofluid from (8) we find $\eta' = 8.7 \times 10^{-15}$ g cm/s in the absence of a magnetic field and $\eta' = 11.4 \times 10^{-15}$ g cm/s in field 150 Oe ($\alpha = 4$). A close estimate of the spin viscosity—$\eta' = 6.4 \times 10^{-15}$ g cm/s—was obtained in a different way by Schumacher *et al.* [24]. Almost all of the previous estimates were based on dimensional analysis alone [7,25,26]: The spin viscosity depends on the viscosity of the fluid and some internal length b equal to the distance between the centers of neighboring microeddies, that is, $\eta' \simeq \eta b^2$. But $b \simeq d_h\phi^{-1/3}$ and, therefore, η' tends to infinity in the limit of infinite dilution, which is clearly not true. Rinaldi and Zahn [27] assumed that $\eta' \propto \phi^2$.

C. Magnetic torque that rotates the particles

To the equations of motion (1) and (2) it is necessary to add the equation of the ferrofluid magnetization. As such, we use the so-called third magnetization equation [28],

$$\frac{d\boldsymbol{\mathcal{H}}}{dt} = \boldsymbol{\omega} \times \boldsymbol{\mathcal{H}} - \frac{1}{\tau}(\boldsymbol{\mathcal{H}} - \mathbf{H}), \quad \mathbf{M} = M_{\rm sat}\mathcal{L}(\alpha)\frac{\boldsymbol{\mathcal{H}}}{\mathcal{H}}, \quad \alpha = \frac{m\mathcal{H}}{kT}, \tag{10}$$

which is easier than others, and almost as accurate even when far from equilibrium. It links the real $\mathbf{H}$ and effective $\boldsymbol{\mathcal{H}}$ magnetic fields. The latter fully determines the fluid magnetization by the Langevin function $\mathcal{L}(\alpha) = \coth\,\alpha - \alpha^{-1}$. Both $\mathbf{H}$ and $\boldsymbol{\mathcal{H}}$ rotate around polar axis z with the same frequency $\boldsymbol{\gamma}$, but the magnetization lags behind the applied magnetic field in phase by an angle θ, which depends on the Brownian rotational diffusion time $\tau = 3\eta V/kT$ where $V = \pi d_h^3/6$. After substituting $d\boldsymbol{\mathcal{H}}/dt = \boldsymbol{\gamma} \times \boldsymbol{\mathcal{H}}$ in Eq. (10), we find $\mathcal{H} = H\,\cos\,\theta$ and the tangent of the angle losses

$\tan\theta = (\gamma - \omega)\tau$ so that the density of the magnetic torque acting on the particles takes the form

$$\mathbf{M}\times\mathbf{H} = M\mathcal{H}\tau(\boldsymbol{\gamma}-\boldsymbol{\omega}) = 2\zeta\alpha\mathcal{L}(\alpha)(\boldsymbol{\gamma}-\boldsymbol{\omega}), \quad \zeta = \tfrac{3}{2}\eta\phi. \tag{11}$$

In the next subsection, we will show that the direct transformation of microscopic vortices into visible fluid motion does not actually occur due to the extremely low spin viscosity. However, there are other effects that do not depend on the spin viscosity but in which the spin of the particles manifests itself quite clearly.

Let us indicate the explicit expressions describing the friction forces acting on the cylinder wall and the release of heat in microeddies. At $\eta' = 0$, the steady-state equations corresponding to Eqs. (1) and (2) have the solution $\mathbf{u} = \boldsymbol{\Omega} = 0$ and $(\mathbf{M}\times\mathbf{H}) = 4\zeta\boldsymbol{\omega}$. Substituting the latter in (11), we obtain

$$\boldsymbol{\omega} = \boldsymbol{\gamma}\Gamma(\alpha), \quad \mathbf{M}\times\mathbf{H} = 4\zeta\boldsymbol{\gamma}\Gamma(\alpha) = 6\eta\phi\boldsymbol{\omega}, \quad \tan\theta = \gamma\tau[1-\Gamma(\alpha)]. \tag{12}$$

Consequently, the moment of viscous forces acting per unit length of the cylinder is equal to

$$\boldsymbol{\mathcal{N}} = \pi R^2(\mathbf{M}\times\mathbf{H}) = 4\pi R^2\zeta\,\boldsymbol{\omega}. \tag{13}$$

It should be emphasized that macroscopic motion in the cylinder is not required for the existence of viscous torque: The latter is the result of microeddies. The average rate of energy dissipation inside these eddies, contained in a unit volume, is determined by the relation,

$$q \equiv -\overline{\mathbf{M}\cdot\dot{\mathbf{H}}} = \boldsymbol{\gamma}\cdot(\mathbf{M}\times\mathbf{H}) = 4\zeta\gamma\,\omega. \tag{14}$$

The release of heat in microvortices causes an increase in temperature, which makes the magnetization of the fluid inhomogeneous over the cross section of the cylinder. The resulting ponderomotive forces are capable of rotating the fluid as will be shown in Sec. IV so that spin viscosity becomes unnecessary.

D. Effect of spin viscosity on ferrofluid rotation

The very concept of internal rotation implies an excess $\boldsymbol{\Lambda} = \boldsymbol{\omega} - \boldsymbol{\Omega}$ of the latent spin over the apparent fluid rotation. In the case of equilibrium, $\boldsymbol{\omega} = \boldsymbol{\Omega}$, there is no internal rotation: Particles do not rotate relative to the surrounding fluid. Therefore, on the inner wall of the cylinder it is natural to set the boundary condition $\boldsymbol{\Lambda} = 0$. Due to the axial symmetry of the problem, only z components of Eqs. (4) and (5) are nontrivial in the steady state,

$$\frac{d}{dr}\left(r\frac{d}{dr}\right)(\eta\,\Omega - \zeta\,\Lambda) = 0, \tag{15}$$

$$\frac{\eta'}{r}\frac{d}{dr}\left(r\frac{d\omega}{dr}\right) - 4\zeta\Lambda + [\mathbf{M}\times\mathbf{H}]_z = 0. \tag{16}$$

From (15) it follows $\Omega = (\zeta/\eta)\Lambda + C$ so that $\omega \equiv \Omega + \Lambda = (1+\zeta/\eta)\Lambda + C$, where C is a constant. Substitution of this ω and $[\mathbf{M}\times\mathbf{H}]_z$ from (11) into (16) gives

$$\Lambda'' + \Lambda'/r - \kappa^2\Lambda = -\kappa_0^2 K(\gamma - C), \quad \kappa_0^2 = \frac{4\zeta\eta}{\eta_e\eta'}, \quad \kappa^2 = \kappa_0^2\left(1 + \frac{\eta_e}{\eta}K\right), \tag{17}$$

$$\eta_e = \eta + \zeta, \quad K = \frac{1}{2}\alpha\mathcal{L}(\alpha) = \frac{\Gamma(\alpha)}{1-\Gamma(\alpha)}. \tag{18}$$

The solution of this equation satisfying the condition $\Lambda(R) = 0$ is

$$\Lambda(r) = \frac{\kappa_0^2}{\kappa^2}K(\gamma - C)\left(1 - \frac{I_0(\kappa r)}{I_0(\kappa R)}\right), \tag{19}$$

where $I_0(\kappa r)$ is the modified Bessel function. The azimuthal fluid velocity is determined by integrating the vorticity $2\Omega = (ru)'/r$,

$$u(r) = \frac{2}{r}\int \Omega(r) r\, dr = \frac{2}{r}\int \left(\frac{\zeta}{\eta}\Lambda(r) + C\right) r\, dr,$$

and finding the constant C from the boundary condition $u(R) = 0$. The exact solution reads

$$u(r) = \frac{\zeta}{\eta}\gamma R\Gamma(\alpha)\frac{\Delta}{\varrho}\left(\frac{r}{R} - \frac{I_1(\kappa r)}{I_1(\kappa R)}\right), \tag{20}$$

$$\Omega(r) = \frac{\zeta\,\gamma}{\eta\,\varrho}\,\Gamma(\alpha)\left(\Delta - \frac{I_0(\kappa r)}{I_0(\kappa R)}\right), \quad \omega(r) = \frac{\gamma}{\varrho}\,\Gamma(\alpha)\left(1 + \frac{\zeta}{\eta}\Delta - \frac{\eta_e}{\eta}\,\frac{I_0(\kappa r)}{I_0(\kappa R)}\right), \tag{21}$$

where

$$\varrho = 1 + \frac{\zeta}{\eta}\Gamma(\alpha)\Delta = 1 + O(\Delta), \quad \Delta = \frac{2I_1(\kappa R)}{\kappa R I_0(\kappa R)} \simeq \frac{2}{\kappa R}\left(1 - \frac{1}{2\kappa R}\right) \quad \text{for } \kappa R > 15.$$

Thus, the fluid velocity is positive over the entire cross section of the cylinder so that the field and fluid rotate in the same direction. The velocity value strongly depends on the diffusion length κ^{-1}. Substituting of η' from (8) into (18) gives

$$\kappa_0^2 = \frac{60\rho}{\hat{\rho}(1 + 1.5\phi)d_h^2}, \quad \kappa^2 = \kappa_0^2[1 + (1 + 1.5\phi)K].$$

For the indicated cobalt-ferrite ferrofluid with $d_h = 39$ nm, $\phi = 24\%$, $\hat{\rho}/\rho = 1.2$ at $\alpha = 4$ [then $\Gamma(4) = 0.6$] and the radius $R = 2$ cm, we get

$$\kappa R = 10.6\left(\frac{R}{d_h}\right) = 5.4 \times 10^6, \quad \Delta = \frac{2}{\kappa R} = 3.7 \times 10^{-7}. \tag{22}$$

So the argument of Bessel functions is huge. From their asymptotic for $\kappa R > \kappa r \gg 1$,

$$\frac{I_n(\kappa r)}{I_n(\kappa R)} = \exp[-\kappa(R - r)],$$

it follows that the gradients of $u(r)$, $\Omega(r)$, and $\omega(r)$ are concentrated in a very narrow layer of thickness $R - r_m$ adjacent to the cylinder wall,

$$r_m = R(1 - \delta), \quad \delta = \frac{\ln(\kappa R)}{\kappa R} \ll 1.$$

For $\kappa R \sim 10^6$ the thickness $R\delta$ is a fraction of a micron. Velocity (20) has a maximum at $r = r_m$ [29] and a linear profile almost to the wall itself (similar to that shown below in Fig. 4). As can be seen from (21), both the spin velocity ω and vorticity Ω are positive over the entire section with the exception of a thin layer of thickness $3\phi/2\kappa$ at the wall cylinder where they are negative,

$$\omega(R) = \Omega(R) = -\frac{\zeta\,\gamma}{\eta\,\varrho}\Gamma(\alpha)(1 - \Delta) \approx -\frac{3}{2}\phi\gamma\Gamma(\alpha). \tag{23}$$

However, this does not result in the reverse flow described in Ref. [30]. The spin velocity remains constant equal to ω from (12) on the interval $0 < r < r_m$ and then drops to the boundary value (23), whereas the angular velocity of the fluid $\Omega(r)$ as well as its linear velocity $u(r)$ are positive and negligible across the entire section.

We also solved the problem by changing the boundary condition from $\omega(R) = \Omega(R)$ to $\omega(R) = 0$. Let us compare the results. In the lowest approximation in Δ, expressions (20) and (21) obtained for the previous boundary condition have the form

$$u(r) = \frac{\zeta}{\eta}\gamma R\Gamma(\alpha)\Delta\left(\frac{r}{R} - \frac{I_1(\kappa r)}{I_1(\kappa R)}\right), \quad \omega(r) = \gamma\Gamma(\alpha)\left(1 - \frac{\eta + \zeta}{\eta}\,\frac{I_0(\kappa r)}{I_0(\kappa R)}\right), \tag{24}$$

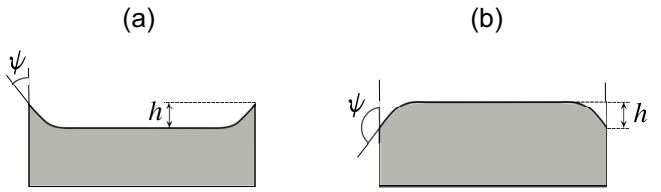

FIG. 3. The (a) concave and (b) convex profiles of the free surface of the ferrofluid. The contact angles are $\psi = 45^\circ$ and $\psi = 135^\circ$, correspondingly. (a) The *concave* shape produces counter-rotation, (b) *convex*—corotation.

and for the last condition we find

$$u(r) = \frac{\zeta}{\eta + \zeta}\gamma R\Gamma(\alpha)\Delta\left(\frac{r}{R} - \frac{I_1(\kappa r)}{I_1(\kappa R)}\right), \quad \omega(r) = \gamma\Gamma(\alpha)\left(1 - \frac{I_0(\kappa r)}{I_0(\kappa R)}\right). \tag{25}$$

In the first case [see (24)], corresponding to boundary conditions (23), magnetic grains in a thin layer near the cylinder wall revolve against the direction of rotation of the field and fluid: $\omega < 0$. This means that the particles *roll* along the cylinder wall in the direction of the fluid motion with almost the same angular velocity since in this thin layer $\omega \approx \Omega$. Such rotating particles do not impede the fluid flow as stationary particles do under the boundary condition $\omega = 0$. As a consequence, under the first boundary condition, the fluid rotates slightly faster than under the second.

For the specified Co-ferrite ferrofluid in a field $H = 150$ Oe rotating at a frequency of $\gamma/2\pi = 500$ Hz, the maximum speed resulting from (24) is

$$u(r_m) \simeq \frac{3\phi\gamma\Gamma(\alpha)}{\kappa} = 5.0 \times 10^{-4}\,\text{cm/s} = 5\ \mu\text{m/s (sic !)},$$

and period of rotation of the fluid in the cylinder of radius $R = 2$ cm is $\mathcal{T} = 2\pi R/u(r_m) = 7$ h. Thus, if the fluid really rotates with a noticeable, i.e., $\gtrsim 1$ cm/s, velocity, then this motion cannot be described within the framework of the theory of spin diffusion due to the vanishingly low spin viscosity.

III. THE ROLE OF FREE SURFACE SHAPE IN THE SPIN-UP PHENOMENON

Rosensweig *et al.* [15] wrote (authors italics): "When the surface is concave the fluid rotates counter to the field; when the surface is flat rotation ceases; and when the surface is convex the fluid rotates in the direction of the field. *This observed behavior indicates that surface stress rather than volumetric stress is responsible for the spin-up phenomenon*." More precisely, surface stresses are responsible for spin-up in a thin surface layer, whereas volume stresses cause this phenomenon in the bulk. That is, different mechanisms are involved here. The height h to which the fluid rises at the hydrophilic wall of a cylinder or lowers at the hydrophobic one does not exceed 2 to 3 mm. The absence of fluid rotation at $h = 0$ and a change in the direction of rotation with a change in the sign of h indicates the rotation of a *thin surface layer* with a thickness of the order of h. Of course, this layer involves the underlying fluid layers in rotation, but their velocity rapidly decreases with distance z from the free surface. In this section, we will first estimate the azimuthal velocity of the surface layer and then the rate of its deceleration as a function of z.

A. Spin-up on the free surface

In the gravity field, the shape of the liquid surface limited by a vertical wall depends on the capillary constant $a = \sqrt{2\sigma/\rho g}$ (here σ is the surface-tension coefficient) and the angle of contact ψ between the fluid and the wall (Fig. 3). The problem to find the shape of the surface $z = z(r)$ for given values of a and ψ has an exact solution [31] from which it follows that $h = a\sqrt{1 - \sin\,\psi}$ and

$z' = \cot\ \psi$ at the surface of the wall. Nevertheless, the dependence $z(r)$ does not exist in an explicit form. For our needs, however, it suffices to use the plausible approximation of the free surface shape. In the case of a concave meniscus, it will be fine that the function,

$$z(r) = h\frac{\cosh(r/h)}{\cosh(R/h)}, \tag{26}$$

which at $R \gg h$ decreases exponentially from its value h on the wall to $2h\exp(-R/h) \simeq 0$ on the cylinder axis. At $r = R$, function (26) satisfies the condition $z' = \cot\ \psi = 1$ for $\psi = 45^\circ$. This situation is depicted in Fig. 3(a).

Below, we consider the concave profile as an excess of magnetic matter in the near-wall region. This excess is distributed over a layer of thickness h in accordance with formula (26), which leads (in a rotating field) to an additional magnetic torque acting on the fluid in the layer. Multiplying the torque density (12) by $z(r)$ and dividing by h, we obtain

$$\overline{\mathbf{M}\times\mathbf{H}} = 6\eta\phi\boldsymbol{\gamma}\Gamma(\alpha)\frac{\cosh(r/h)}{\cosh(R/h)}. \tag{27}$$

Physically, this result represents the r-dependent density of the magnetic torque acting on a layer of a thickness of h and averaged over this thickness. Substituting torque (27) into Eq. (3), we get the following equation for the azimuthal velocity component:

$$\eta\left(u'' + \frac{u'}{r} - \frac{u}{r^2}\right) = 3\eta\phi\,\gamma\,\Gamma(\alpha)\left(\frac{\cosh(r/h)}{\cosh(R/h)}\right)'. \tag{28}$$

For $R \gg h$, the curvature of the cylinder wall can be neglected. Keeping then only the highest derivative of the velocity, we arrive at the equation,

$$u'' = 3\phi\,\gamma\,\Gamma(\alpha)\left(\frac{\cosh(r/h)}{\cosh(R/h)}\right)'.$$

Integrating it and satisfying the boundary conditions $u(0) = u(R) = 0$, we finally find

$$u(r) = -3\phi\,\gamma h\Gamma(\alpha)\tanh(R/h)\left(\frac{r}{R} - \frac{\sinh(r/h)}{\sinh(R/h)}\right), \tag{29}$$

below $\tanh(R/h) \approx 1 - 2\exp(-2R/h)$ is replaced by 1. The minus sign in front of the right-hand side of (29) means the opposite rotation of the field and fluid. It is noteworthy that the rotational speed of a thin surface layer of a ferrofluid does not depend on its viscosity.

In the case of the convex shape of the free surface, we replace (26) by the function,

$$z(r) = h\left(1 - \frac{\cosh(r/h)}{\cosh(R/h)}\right), \tag{30}$$

which satisfies the boundary condition $z' = \cot 135^\circ = -1$ as shown in Fig. 3(b). This change in sign of z' (from $\cot 45^\circ$ to $\cot 135^\circ$) leads to a change in speed to the opposite. Consequently, a ferrofluid with a convex free-surface profile rotates in the same direction as the applied field.

Rosensweig and his colleagues [15] placed a water-based magnetite ferrofluid ($M_d = 450$ G) with $\phi_m \simeq 1\%$ in an open cylindrical vessel with a radius $R = 2.33$ cm and applied to it a rotating magnetic field with an amplitude of $H = 100$–200 Oe at a rotational speed $\gamma/2\pi = 60$ Hz. For pure water the capillary constant $a = 3.8$ mm at 20 °C, but surfactants used to stabilize magnetic colloids greatly reduce their surface tension [25]. Taking $\sigma = 20$ erg/cm^2 (see Table 2.4 in Ref. [25]), we obtain the capillary constant $a \approx 2$ mm and the surface deformation $h = a\sqrt{1 - \sin 45^\circ} \approx 1$ mm. Due to the smallness of h, the velocity (29) reaches its maximum value $u(r^*)$ in the immediate vicinity of the cylinder wall,

$$\frac{r^*}{R} = 1 - \frac{\ln(R/h)}{(R/h)} = 0.865, \quad u(r^*) = -3\phi\,\gamma h\Gamma(\alpha)\left(1 - \frac{\ln(eR/h)}{(R/h)}\right).$$

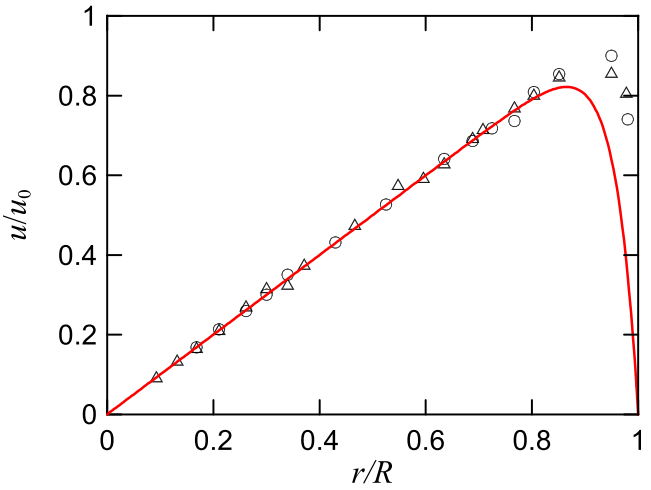

FIG. 4. The azimuthal velocity of the ferrofluid surface in a cylinder of $R = 2.33$ cm, $\gamma/2\pi = 60$ Hz. The symbols mark the experimental data: ◯ $-H = 100$ Oe, △ $-H = 200$ Oe [15], and the solid line is described by the expression (31). The maximum point on this curve has coordinates $r^*/R = 0.865$ and $u(r^*)/u_0 = 0.822$.

The authors of Ref. [15] introduced the velocity $u_0 = -3\phi\gamma h\Gamma(\alpha)$, the value of which follows from $u(r^*)$ in the limit $h \to 0$, representing the result of linear extrapolation of $u(r)$ up to the wall. For the sample and field parameters indicated above, the ratio,

$$\frac{u(r)}{u_0} = \frac{r}{R} - \frac{\sinh(r/h)}{\sinh(R/h)} \tag{31}$$

is presented in Fig. 4 where experimental velocity profiles [15] are shown by symbols for two field amplitudes. Almost solid-body fluid rotation in the core and the thinness of the near-wall layer allow us to interpret the ratio $\Omega_0 = |u_0|/R$ as the characteristic angular velocity of the fluid. In agreement with the experimental data [15], Ω_0 proves to be inverse to R.

Above, we neglected the curvature of the cylinder wall and kept only the highest-order derivative on the left side of Eq. (29). It is worth noting that keeping all the terms in this equation, we arrive at the same its solution with the replacement of $\cosh(r/h)$ and $\sinh(r/h)$ correspondingly by $I_0(r/h)$ and $I_1(r/h)$. Then both velocity profiles determined by formula (29) before and after this change are completely indistinguishable in Fig. 4. Amusingly, this replacement makes the expression (29) similar to Eq. (21) with κ replaced by h^{-1}. This similarity is nothing more than a consequence of the cylindrical symmetry of both problems. Indeed, the velocity (29) was obtained for $\eta' = 0$, that is, outside the scope of the spin-diffusion theory. Note that even length scales are incommensurable: $h \sim 10^{-1}$ versus $\kappa^{-1} \sim 10^{-7}$ cm.

B. How deep does the rotation of the surface penetrate into the bulk?

The rotation of the thin surface layer makes it rotate fluid that is below. The similar situation has long been known as the Kármán problem (1921): An infinite disk rotates in an unbounded volume of viscous fluid on the plane $z = 0$ about the z axis with the angular velocity Ω. Exact self-similar solution of the problem determines the azimuthal velocity $v_\varphi = r\Omega G(\xi)$ proportional to the distance r from the axis of rotation—just as in Fig. 4—and depending on the dimensionless axial coordinate $\xi = z\sqrt{(\Omega/\nu)}$ where $\nu = \eta/\rho$ is the kinematic viscosity. Figure 5 demonstrates that the function $G(\xi)$ is well approximated (especially for $\xi > 1.5$) by the exponent $G(\xi) = \exp(-\xi/1.3)$.

We define the characteristic penetration length z^* as the distance from the disk at which the angular velocity of the fluid v_φ/r falls from Ω at $z = 0$ to $0.1\,\Omega$. The equality $\exp(-\xi^*/1.3) =$

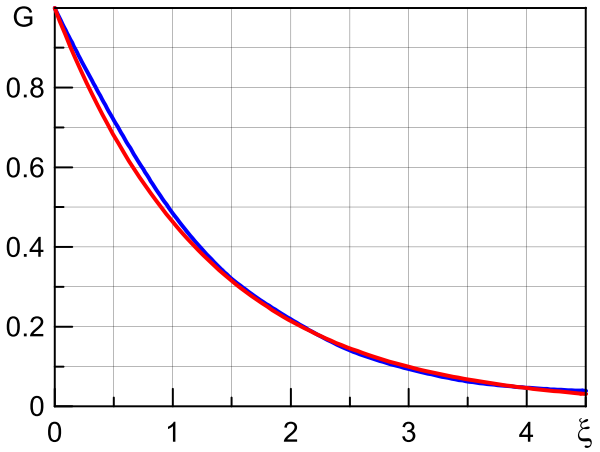

FIG. 5. Nondimensional azimuthal velocity G in the Kármán problem as a function of $\xi = z\sqrt{\Omega/\nu}$. The *blue curve* taken from Fig. 7 in Ref. [31] is the exact solution; the *red curve*—our approximation by the function $G = \exp(-\xi/1.3)$.

0.1 determines the dimensionless distance $\xi^* = 3$, thus, $z^* = 3\sqrt{\nu/\Omega}$ (note that z^* increases with increasing fluid viscosity since it is the viscosity forces that transfer rotation from the upper layers of the fluid to the lower ones). For a slowly rotating disk, $\Omega = 0.2\pi$ s^{-1} (i.e., $\Omega = 6$ rpm) and $\nu = 0.01$ cm^2/s (water) we get $z^* = 3.8$ mm. In the experiment [15], there were $\Omega_0 = \frac{1.50 \text{ cm/s}}{2.33 \text{ cm}} = 0.644$ s^{-1} $= 6.15$ rpm and $\nu = 0.03$ cm^2/s, that results in $z^* = 6.5$ mm. This estimate is consistent with measurements by Lebedev and Pshenichnikov [32]: "the fluid motion is concentrated in the thin layer ($\sim R/4$) adjoining the surface;" their cylinder had a diameter of 47 mm.

The above estimate is obtained without considering the edge effects: The radius R of cylinder is finite, whereas the solution to the Kármán problem is obtained for an infinite disk. In our geometry, one of the edge effects is the energy dissipation due to friction against the cylinder wall. Allowing for this additional dissipation would only decrease the value of z^*. However, even without such a correction, it is clear that the magnetic torque arising on a curved free surface cannot induce a flow in the bulk.

IV. SPIN-UP CAUSED BY THE THERMAL EFFECT

The dissipation of energy in microvortices leads to heating of the ferrofluid. In a rapidly rotating magnetic field, this heating may be sufficient to induce the spin-up phenomenon as was first indicated in Ref. [33]. Then this topic was developed and investigated experimentally in a series of works by Lebedev and Pshenichnikov [20], Pshenichnikov [34], and Pshenichnikov *et al.* [35].

A. Temperature profile and azimuthal velocity

The rotation of magnetic particles in a viscous fluid creates internal heat sources, the volumetric density of which q is determined by the relation (14). The heat transfer equation, $\nabla^2 T = -q/\lambda$, predicts the parabolic temperature profile,

$$T(r) = T(R) + \Theta\left(1 - \frac{r^2}{R^2}\right), \quad \Theta = \frac{qR^2}{4\lambda} = \frac{3}{2\lambda}\eta\phi\gamma^2 R^2 \Gamma(\alpha), \tag{32}$$

where Θ is the temperature difference between the axis and the cylinder wall, λ is the heat conductivity, and $\Gamma(\alpha)$ is defined in (9). Temperature inhomogeneity makes ρ, $\mathbf{M}$, and $\mathbf{H}$ functions

of r, so the Archimedes and Kelvin forces must be included in Eq. (3),

$$\eta\nabla^2\boldsymbol{u} + (\mathbf{M}\nabla)\mathbf{H} + \tfrac{1}{2}\nabla\times(\mathbf{M}\times\mathbf{H}) - \rho\,\mathbf{g}\beta T = \nabla p, \tag{33}$$

here $\mathbf{g}$ is the gravity acceleration, and β is the coefficient of thermal expansion. The magnetization $\mathbf{M} = (M/\mathcal{H})\boldsymbol{\mathcal{H}}$ depends on the effective field $\boldsymbol{\mathcal{H}}$ which lags behind the internal field $\mathbf{H}$ by an angle θ: $\mathcal{H} = H\,\cos\,\theta$ (see Sec. II C). In a cylindrical frame of reference with unit vectors $\hat{\boldsymbol{r}}, \hat{\boldsymbol{\varphi}}, \hat{\boldsymbol{z}}$, which revolves around the z axis with the frequency γ of the magnetic field, direct $\hat{\boldsymbol{r}}$ along the magnetization: $\boldsymbol{\mathcal{H}} = \mathcal{H}\hat{\boldsymbol{r}}$. Then the above equality, $H = \mathcal{H}/\cos\,\theta$, written as $H^2 = \mathcal{H}^2(1+\tan^2\theta)$, can be expanded as $\mathbf{H} = \mathcal{H}\hat{\boldsymbol{r}} \pm \mathcal{H}\,\tan\,\theta\hat{\boldsymbol{\varphi}}$. The correct sign (minus) in front of the last term in this expression is determined from Maxwell's equation for a nonconductive material $\nabla\times\mathbf{H} = 0$. Satisfying it, we put $\mathbf{H} = \nabla\Phi$ with the magnetic potential $\Phi = Hr\,\cos\,\varphi$, which in our case leads to $H_r = H\,\cos\,\theta = \mathcal{H}$ and $H_\varphi = -H\,\sin\,\theta = -\mathcal{H}\,\tan\,\theta$. Substitution of the components $\mathbf{M}$ and $\mathbf{H}$ into the density of the Kelvin force gives

$$(\mathbf{M}\nabla)\mathbf{H} = M\nabla\mathcal{H} - \hat{\boldsymbol{\varphi}}M\frac{d}{dr}(\mathcal{H}\,\tan\,\theta).$$

The first term on the right side can be represented as the gradient of the r function and combined with the pressure gradient. The second term together with

$$\frac{1}{2}[\nabla\times(\mathbf{M}\times\mathbf{H})]_\varphi = -\frac{1}{2}\frac{d}{dr}(MH\,\sin\,\theta) = -\frac{1}{2}\frac{d}{dr}(M\mathcal{H}\,\tan\,\theta)$$

gives the azimuthal component of the force density $F_\varphi(r)$, which exactly causes the spin-up flow,

$$\eta\left(u'' + \frac{u'}{r} - \frac{u}{r^2}\right) + F_\varphi(r) = 0 \quad \text{where} \quad F_\varphi = -\frac{1}{2}\frac{d}{dr}(M\mathcal{H}\,\tan\,\theta) - M\frac{d}{dr}(\mathcal{H}\,\tan\,\theta). \tag{34}$$

Substituting here $M = nm\mathcal{L}(\alpha)$, $\tan\,\theta = 2\gamma\tau/[2+\alpha\mathcal{L}(\alpha)]$, and $\tau = 3\eta V_h/kT$, we obtain this force in the form

$$F_\varphi = -3\eta\phi\gamma\left[\frac{\partial}{\partial\alpha}\left(\frac{\alpha\mathcal{L}}{2+\alpha\mathcal{L}}\right) + 2\mathcal{L}\frac{\partial}{\partial\alpha}\left(\frac{\alpha}{2+\alpha\mathcal{L}}\right)\right]\frac{\partial\alpha}{\partial T}\frac{dT}{dr}, \tag{35}$$

where $\mathcal{L} \equiv \mathcal{L}(\alpha)$. Finally, substituting $\partial\alpha/\partial T = -\alpha/T$ and $T' = -2\Theta r/R^2$ in (35) gives

$$F_\varphi = -\frac{18\eta^2\phi^2\gamma^3}{\lambda T}f(\alpha)r, \quad f(\alpha) = \frac{\alpha^2\mathcal{L}}{(2+\alpha\mathcal{L})^3}[\mathcal{L} + \alpha(1+\mathcal{L}^2) - \alpha^2\mathcal{L}(1-\mathcal{L}^2)]. \tag{36}$$

Equation (34) with F_φ from (36) has the solution,

$$u(r) = -u_0\frac{r}{R}\left(1 - \frac{r^2}{R^2}\right), \quad u_0 = \frac{9\eta\phi^2\gamma^3R^3}{4\lambda T}f(\alpha). \tag{37}$$

Here the minus before u_0 means the opposite rotation of the field and fluid. The speed reaches its maximum at $r = R/\sqrt{3}$; the linear and angular velocities at this point are

$$u_\mathrm{m} \equiv |u(R/\sqrt{3})| = \frac{\sqrt{3}\,\eta\phi^2\gamma^3R^3}{2\lambda T}f(\alpha), \quad \Omega_\mathrm{m} \equiv \Omega(R/\sqrt{3}) = \frac{\sqrt{3}u_\mathrm{m}}{2\pi R}. \tag{38}$$

The dependencies of Θ and u_m on the Langevin parameter are shown in Fig. 6. The temperature difference $\Theta(\alpha)$ between the axis and the wall of the cylinder starts at $\alpha^2/6$ for small α and then tends to saturation as $(1-2/\alpha)$. The dependence of $u_\mathrm{m}(\alpha)$ is more interesting. On the initial portion of the red curve, the velocity rises as $\alpha^4/18$. This result $u_\mathrm{m} \propto H^4$ was obtained by Pshenichnikov [34] without using any magnetization equation. In a weak magnetic field, $\mathbf{M}$ and $\mathbf{H}$ are related by a simple linear equation through the complex dynamic susceptibility. Its real and imaginary parts can be measured experimentally, so their temperature dependence is considered known. Such an approach implemented in Refs. [34,35] brings $u_\mathrm{m} = 0.1$ mm/s in agreement with experimental

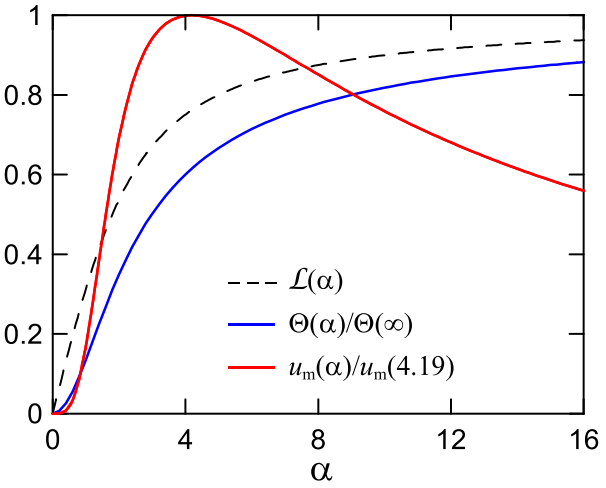

FIG. 6. Dependence on the Langevin parameter of the temperature difference Θ between the axis and the cylinder wall, and the maximum speed u_m of fluid rotation; *dashed line*, relative magnetization $\mathcal{L}(\alpha) = M(\alpha)/M_{sat}$.

results presented in Ref. [20]. As seen in Fig. 6, the fluid velocity remains insignificant at $\alpha \leqslant 0.8$ [36] but at $\alpha \geqslant 2$ takes quite observable values pointed in Table I.

The red curve reaches its maximum at $\alpha = 4.19$ and then decreases as $2/\alpha$. This fall is a consequence of the saturation of the fluid magnetization. For large α, when $\mathcal{L}(\alpha) \approx 1 - \alpha^{-1}$, the difference between the magnetization on the cylinder wall and its axis $\delta M = M(R) - M(0)$ decreases with the field growth,

$$\frac{\delta M}{M} = \frac{\mathcal{L}(\alpha_R) - \mathcal{L}(\alpha_0)}{\mathcal{L}(\alpha)} = \alpha_0^{-1} - \alpha_R^{-1} = \frac{k\Theta}{m\mathcal{H}} = \frac{\Theta/T}{\alpha}.$$

Thus, at $\alpha \gg 1$, the magnetization becomes *uniform* across the entire section of the cylinder, which means that the very reason for the spin-up effect disappears.

The left half of Table I shows the parameters of a Co-ferrite ferrofluid close in properties to WBF-2 from Ref. [19] and the amplitude and frequency of the rotating field. The effects caused by this field take up the right half of the table. They include the tangent of the loss angle (12), the temperature difference Θ, the maximum linear (u_m), and angular (Ω_m) velocities, and the Grashof number (43), which characterizes the intensity of thermal convection.

TABLE I. Parameters of a Co-ferrite ferrofluid and the results of calculations.[a]

M_{sat} (G)	α	$\gamma/2\pi$ (Hz)	R (cm)	ϕ (%)	η (cP)	tan θ	Θ (K)	u_m (cm/s)	Ω_m (rpm)	Gr
8.5	2.0	400	2.0	24	2.7	0.101	1.4	1.1	9.3	5470
8.5	2.5	400	2.0	24	2.8	0.091	1.8	1.4	12	6120
8.5	3.0	500	1.7	24	2.9	0.104	2.5	2.0	19	5190
10.6	3.0	300	2.0	30	3.7	0.079	2.0	1.4	12	4550
12.8	4.0	200	2.0	36	7.3	0.084	2.5	1.8	15	1630

[a]Domain magnetization $M_d = 425$ G, Langevin parameter $\alpha = 2$ for $H = 70$ Oe, particle magnetic core $d_m = 17$, $d_h = 39$ nm, $\phi = (d_h/d_m)^3\phi_m = 12\,\phi_m$, thermal conductivity $\lambda = 6 \times 10^4$ g cm s^{-3} K^{-1}, thermal expansion $\beta = 3 \times 10^{-4}$ K^{-1}, viscosity was calculated by Eq. (9), Gr—the Grashof number (43).

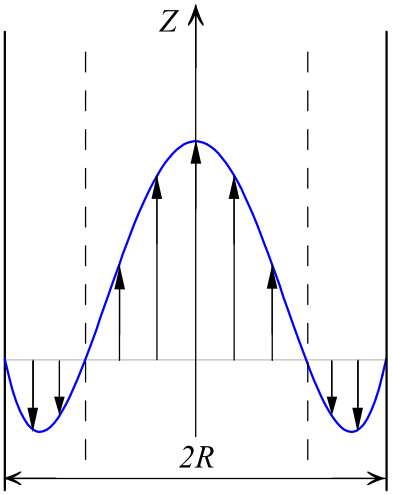

FIG. 7. Convective flow structure caused by internal heat sources in a long cylinder closed at the top and bottom. The *dashed line*—the interface between ascending and descending flows.

B. Allowance for natural convection

Internal heating of the fluid causes gravitational convection. Substitution of $T(r)$ from (32) into Eq. (34) gives the following equation for the vertical component of the fluid velocity $v(r)$:

$$\eta v'' + \rho g \beta \Theta \left(1 - \frac{r^2}{R^2}\right) = \frac{dp}{dz} = C, \tag{39}$$

where C is the separation-of-variables constant. The velocity vanishes at the cylinder wall. In addition, we assume that the cylinder is closed at the top and bottom, which means that the flow through any cross section of the cylinder is zero,

$$v(R) = 0, \quad \int_0^R v(r) r\, dr = 0. \tag{40}$$

From (39) and (40) it follows:

$$v(r) = v_0 \left(1 - 4\frac{r^2}{R^2} + 3\frac{r^4}{R^4}\right) = v_0 \left(1 - \frac{r^2}{R^2}\right)\left(1 - 3\frac{r^2}{R^2}\right), \quad v_0 = \frac{g\beta\Theta R^2}{48\nu}, \tag{41}$$

where $\nu = \eta/\rho$ is the kinematic viscosity. The velocity profile is shown in Fig. 7. As seen, the cylindrical interface $r_0 = R/\sqrt{3}$ separates the ascending (axial) and descending (near-wall) flows. In both of these sectors, due to the azimuthal component of the velocity, the trajectory of each fluid element is a helix with a pitch L depending on r: the ratio (37) to (41) gives

$$L(r) = 2\pi r \frac{v(r)}{u(r)} = L_0 \left(1 - 3\frac{r^2}{R^2}\right), \quad L_0 = \frac{\pi}{36} \frac{g\beta T R^2 \Gamma(\alpha)}{\gamma \nu \phi f(\alpha)}. \tag{42}$$

In the points of maximum of $v(r)$ in ascending ($r_\uparrow = 0$) and descending ($r_\downarrow = R\sqrt{2/3}$) flows, we find the values $L = \pm L_0$, respectively. For the case presented in the second row of Table I, we get $L_0 = 5.7$ cm, and similarly $L_0 = 2.8$ cm for the fifth row. As can be seen from these estimates, the vertical and azimuthal velocity components are quite comparable with each other: $v/u \sim L_0/R \sim 1$. It is curious that at the interface $r_0 = R/\sqrt{3}$ where the vertical velocity of the fluid is zero, its azimuthal component has a maximum, $u(r_0) = u_\mathrm{m}$—see Eq. (38). If the field rotates clockwise, then the streamlines are right-handed helices in the axial region $r < r_0$, left-handed helices at the

periphery $r_0 < r < R$, and vice versa, if the field rotates counterclockwise. Only fluid elements located at the interface between convective counter-currents move along circular paths.

It is important that the two-dimensional flow $\mathbf{u} = (0, u, v)$ preserves (due to the absence of the r component of velocity) the temperature profile (32) and, therefore, does not in any way affect the spin-up phenomenon. However, this situation arises only at subcritical values of the dimensionless parameter—the Grashof number,

$$\mathrm{Gr} \equiv \frac{g\beta\Theta R^3}{\nu^2} = \frac{g\beta q R^5}{4\nu^2\lambda}, \tag{43}$$

which approximates the ratio of buoyancy to the force of viscosity acting on the fluid. It is analogous to the Reynolds number $\mathrm{Re} = v_0 R/\nu$: Substitution of the velocity amplitude v_0 from (41) into this expression gives $\mathrm{Re} = \mathrm{Gr}/48$. As seen, for a given density q of internal heat sources, Gr strongly depends on the radius of the cylinder.

The two-dimensional convective motion shown in Fig. 7 becomes unstable at some critical value of $\mathrm{Gr_c}$. The instability originates on the counterflow interface and develops at $\mathrm{Gr} > \mathrm{Gr_c}$ in the form of a system of vortices on the r-z plane of Fig. 7. Such vortices mix the liquid, smoothing the temperature distribution (32) over the cylinder cross section and thereby decreasing the spin-up speed. The stability of plane-parallel convective flow in a vertical slit due to internal heat sources was studied by Gershuni *et al.* [37]. Using their results, we estimated the critical Grashof number for the geometry under consideration; we found $\mathrm{Gr_c} \approx 6800$.

V. DISCUSSION AND CONCLUDING REMARKS

Returning to the theory of spin diffusion, we note that the spin viscosity determines the characteristic diffusion length $\kappa^{-1} \sim \sqrt{\eta'/6\eta\phi}$, the value of which limits the applicability of this theory to explain the spin-up phenomenon. This limit looks as $\kappa R \lesssim 30$, that is, κ^{-1} should be *comparable* with the radius of cylinder R. Probably, this condition is fulfilled when water flows through *nanotubes* [38–40] in a rotating electric field. Hansen *et al.* [39] found the estimate $\kappa^{-1} \simeq 2$ nm. Thus, $\kappa R = 5$ for $R = 10$ nm and $\kappa R = 20$ for $R = 40$ nm. However, in the case of a ferrofluid, we are dealing with macroscopic samples, $R \sim 1$ cm when $\kappa R \sim 10^6$. For such huge values due to the negligible η', the theory predicts no flow.

Striking discrepancies in the spin viscosity estimates arise when trying to describe the experimental velocity profiles $u(r)$ by expression (20) using κ as a fitting parameter. According to (22), the dimensionless quantity $\kappa R \simeq 10R/d_h$, so for $R = 2.5$ cm and $d_h = 40$ nm one obtains $\kappa R \simeq 6 \times 10^6$. This value is vary far from $\kappa R = 0.44$ (Torres-Diaz *et al.* [19]), from $\kappa R = 1.319$ (Felderhof [41]), and even from $\kappa R = 100$ (Chaves *et al.* [17]). Because of this, the spin viscosity coefficient, which is inversely proportional to κ^2, turns out to be overestimated by many orders of magnitude. Finlayson [12] gives many examples of this exaggeration of η'.

Brown and Horsnell [13] and Mailfert and Martinet [42] reported changing the direction of the fluid rotation from positive (corotation with the field) to negative (counter-rotation) taking place with growth of the magnetic field. Mailfert and Martinet note that a concave meniscus "corresponding to an excess of [magnetic] grains on the outside [i.e., near the wall, such as in Fig. 3(a)] shows negative rotation." On the contrary, a convex meniscus corresponding to the deficit of particles at the wall and their excess around the cylinder axis [such as in Fig. 3(b)] shows positive rotation. Mailfert and Martinet [42] propose the following explanation of the transition from positive to negative fluid rotation: "When there is an initial positive rotation, the centrifugal force tends to accumulate the grains at the outside: This leads then to a negative rotation for the central part. This rotation stabilizes itself because the centrifugal force maintains the same sign for the concentration gradient which caused it."

This explanation is unsatisfactory as can be seen from a simple estimate of the radial drift velocity of particles v under the action of centrifugal and Stokes forces: $\mu u^2/R \sim 3\pi\eta d_h v$, where μ stands for the particle mass and u is its azimuthal velocity. For $u \sim 1$ cm/s and $d_h = 40$ nm we find

$v \sim 10^{-10}$ cm/s: the centrifugal force is vanishingly small due to the small size of particles, so that surface forces completely prevail over bulk forces.

Positive rotation of the surface layer in a weak magnetic field is observed only in the case of a convex meniscus. The flow reversal with the field increase is most likely the result of the competition between the above-mentioned surface effect and the volumetric heat release (see Sec. IV). The latter provides counter-rotation, which sharply increases ($\sim\alpha^4$) in the region of weak magnetic fields.

Rosenthal *et al.* [16] measured the friction torque acting on the plastic spindle completely filled with ferrofluid (the absence of a free surface of the fluid is emphasized) and placed in a rotating field. They came to conclusion, that "the measured torque arises due to shear stresses at the fluid/spindle boundary and, hence, is a result of bulk flow in the fluid." This is not exactly the way it is explained below. The torque acting on particles from the field is balanced by the torque of the viscous friction in the microscopic (*not hydrodynamic!*) vortices around the particles. As expected, in the frames of the spin-diffusion theory, the bulk flow adds negligibly to the moment of friction forces (12). Recall that this expression is obtained when $\eta' = 0$, that is, when $\mathbf{u}$ and $\mathbf{\Omega}$ are equal to zero. Substituting $u(r)$ from (24) and (25) in (B1) and using the conditions of continuity of H_φ and B_r on the cylinder wall, we found the friction torque $\mathcal{N}_z = -2\pi R^2 \sigma_{\varphi r}$ [31]. Substituting here the φr component of the stress tensor [see Eq. (B1) in Appendix B], we find

$$\mathcal{N}_z = 4\pi R^2 \zeta \gamma \frac{\alpha \mathcal{L}(\alpha)}{2 + \alpha \mathcal{L}(\alpha)} \left[1 - \frac{2 I_1(\kappa R)}{\kappa R I_0(\kappa R)} \right]. \tag{44}$$

Noteworthy is the fact that both types of boundary conditions for the spin velocity $\omega(R) = \Omega(R)$ and $\omega(R) = 0$, lead to the same result. The first term in square brackets (one) corresponds to friction in microeddies, and the second corresponds to bulk flow. Since $\kappa R \sim 10^6$, the content of the parentheses is indistinguishable from one. Thus, the measurement of the torque acting on the vessel with the ferrofluid does not answer the question about the presence or absence of fluid motion in the vessel.

The main property of the spin-up phenomenon is its high sensitivity to the free-surface deformations as well as to any temperature and magnetic-field inhomogeneities. So, the change in the sign of the surface deformation $h \sim \pm 1$ mm from "plus" to "minus" leads to the replacement of the corotation of the field and fluid with their counter-rotation. As we have shown in Sec. IV and Table I, the typical values of the spin-up velocities $u \sim -1$ cm/s might be due to the temperature difference $\Theta \simeq 2$ K between the cylinder axis and its wall. According to Eqs. (38) and (39), the Langevin parameter $\alpha \sim H/T$ is the tuning parameter of the spin-up effect. Therefore, the same spin-up effect can be achieved using the indicated temperature difference $\Theta \sim 2$ K or a slight inhomogeneity of the magnetic field $\sim 2/300 \approx 0.7\%$.

Torres-Diaz *et al.* [19] wrote that "nonuniformities in the magnetic field intensity were lower than 5% in the radial direction in the midplane of the stator cavity," which is *seven times* larger then it is needed to induce the observable fluid rotation. It is logical to assume that the corotation of the field and the fluid discovered in Ref. [19] arises due to the field inhomogeneities. Note that the velocity profiles shown in Figs. 21–23 work [19] are well described by the expression (37) with a distinct maximum at $r/R = 0.58$ (which is exactly $1/\sqrt{3}$!). Lebedev and Pshenichnikov [20] observed the counter-rotation of the field and fluid. As a source of the magnetic field, they used the crossed Helmholtz coils with negligible (less than 1%) inhomogeneity within the working area.

Let us summarize the research results. First of all, the value of the spin viscosity η' was determined. The latter turned out to be negligible as a result of which the spin-up phenomenon cannot be explained within the framework of the concept of spin diffusion. So we set $\eta' = 0$ and developed a theory relating the rotational motion of the free-surface layer to the shape of the meniscus. Its height (to which the fluid rises or falls at the wall) and the contact angle, together with the amplitude and frequency of the field, determine the direction of fluid rotation, the magnitude of the velocity, and its profile. The results are in good agreement with the experimental data of Rosensweig *et al.* [15]. As for the bulk flow of a ferrofluid, we associate it with the action of ponderomotive forces arising

from inhomogeneities of the magnetic field and magnetization. The case of such inhomogeneities caused by an increase in temperature due to heat release in microvortices is studied in detail.

ACKNOWLEDGMENTS

I thank R. E. Rosensweig for stimulating discussion and K. I. Morozov for support and assistance in this work.

APPENDIX A: TO THE DERIVATION OF RELATION (6)

The difference between the spin velocity on the axis of the cylinder $\omega(0)$ and on its wall $\omega(R)$ leads to the diffusion of $\omega(r,t)$. (The diffusion is provided by internal friction between microeddies of diameter $\sim d$.) Hydrodynamic equations (4) and (5) treat a ferrofluid as a continuous medium, which implies $R \gg d$: In the problem, radius R is the characteristic length scale and, hence, the Laplace operator in these equations $\nabla^2 \sim R^{-2}$.

After turning off the rotating field, Eqs. (4) and (5) take the form

$$\frac{d\mathbf{\Omega}}{dt} = \frac{\eta}{\rho}\nabla^2\mathbf{\Omega} - \frac{I}{4\rho\tau_s}\nabla^2(\boldsymbol{\omega} - \mathbf{\Omega}), \tag{A1}$$

$$\frac{d\boldsymbol{\omega}}{dt} = \frac{\eta'}{I}\nabla^2\boldsymbol{\omega} - \frac{1}{\tau_s}(\boldsymbol{\omega} - \mathbf{\Omega}). \tag{A2}$$

Both of them describe a two-stage decay of rotation of a ferrofluid. This rotation consists of microeddies around rotating particles with a spin velocity ω (their scale is $d \sim 10$ nm) and macroscopic vortices Ω of the size $R \sim 1$ cm. Microeddies relax instantly: ω falls to Ω for the spin-relaxation time $\underline{\tau_s = I/(6\eta\phi)} = \hat{\rho}d^2/(60\eta) \sim 10^{-11}$ s, and since then $\omega = \Omega$, the above equations take the form

$$\frac{d\mathbf{\Omega}}{dt} = \frac{\eta}{\rho}\nabla^2\mathbf{\Omega} \quad \text{and} \quad \frac{d\mathbf{\Omega}}{dt} = \frac{\eta'}{I}\nabla^2\mathbf{\Omega}. \tag{A3}$$

Note that we arrived at (A3) under the assumption that the spin-relaxation time τ_s is much shorter than the spin-diffusion time τ_D, the value of which can be easily estimated using Eq. (A2), where

$$\frac{\eta'}{I}\nabla^2\boldsymbol{\omega} \sim \frac{\eta'}{I}\frac{\omega}{R^2} \equiv \frac{\omega}{\tau_D}, \quad \underline{\tau_D = IR^2/\eta'}. \tag{A4}$$

The inequality $\tau_D \gg \tau_s$ is reduced to

$$\eta' \ll \frac{60\eta I}{\hat{\rho}d^2}R^2, \tag{A5}$$

which for any value of η' can be satisfied by choosing a cylinder of sufficiently large radius R. Then relation (6), which follows from (A3), holds: $\eta' = \eta I/\rho$. Substituting this η' into inequality (A5), we obtain the obvious

$$d^2 \ll (\rho/\hat{\rho})60R^2, \tag{A6}$$

where $\hat{\rho}$ and ρ are densities of the particles and suspension. Thus, relation (6) holds for $R \gg d/8$, which is always true.

APPENDIX B: ON THE SYMMETRY OF THE FERROFLUID STRESS TENSOR

In a rare article on the spin-up effect, the reader does not face a discussion or, at least, mentioning of the stress tensor asymmetry. Let us consider this question.

The stress tensor of ferrofluids [23] and liquid paramagnets [43] consists of two viscous parts (corresponding to macroscopic motion and latent rotation) and a magnetic part (the Maxwell tensor),

$$\sigma_{ik} = -p\delta_{ik} + \eta\left(\frac{\partial v_i}{\partial x_k} + \frac{\partial v_k}{\partial x_i}\right) + 2\zeta(\omega_{ik} - \Omega_{ik}) + \frac{1}{4\pi}\left(H_i B_k - \frac{1}{2}H^2\delta_{ik}\right). \tag{B1}$$

This form is not final yet: Eq. (2) gives a possibility to simplify it. The extreme smallness of the spin-relaxation time indicated in Appendix A makes it possible to omit the inertial term in (2) and then eliminate the excess $(\boldsymbol{\omega} - \boldsymbol{\Omega})$ from (B1),

$$\sigma_{ik} = -\left(p + \frac{1}{8\pi}H^2\right)\delta_{ik} + \eta\left(\frac{\partial v_i}{\partial x_k} + \frac{\partial v_k}{\partial x_i}\right) + \frac{1}{2}(M_i H_k + M_k H_i) + \frac{1}{4\pi}H_i H_k + \frac{\eta'}{2}\frac{\partial^2\omega_{ik}}{\partial x_l^2}. \tag{B2}$$

In Sec. II, we showed how small the spin viscosity is so that the last antisymmetric term in (B2) can be neglected. Nonetheless, we will show—it is important, in principle—that "if a spin viscosity is included...and the stress tensor has an asymmetric portion" (Finlayson [12]), this tensor can always be symmetrized. We emphasize that this is possible even for large η'.

"The proof is an exercise in arithmetic" (Martin *et al.* [44]). Let us replace σ_{ik} from (B2) by

$$\tilde{\sigma}_{ik} = \sigma_{ik} + \frac{\eta'}{2}\frac{\partial}{\partial x_l}\left(\frac{\partial\omega_{kl}}{\partial x_i} + \frac{\partial\omega_{il}}{\partial x_k} - \frac{\partial\omega_{ik}}{\partial x_l}\right). \tag{B3}$$

It is easy to see that the divergences $\partial\sigma_{ik}/\partial x_k$ and $\partial\tilde{\sigma}_{ik}/\partial x_k$, which determine the force F_i, are identical,

$$\frac{\partial\tilde{\sigma}_{ik}}{\partial x_k} - \frac{\partial\sigma_{ik}}{\partial x_k} = \frac{\eta'}{2}\left[\frac{\partial}{\partial x_l}\left(\frac{\partial^2\omega_{kl}}{\partial x_k\partial x_l}\right) + \frac{\partial}{\partial x_k}\left(\frac{\partial^2\omega_{il}}{\partial x_k\partial x_l}\right) - \frac{\partial}{\partial x_l}\left(\frac{\partial^2\omega_{ik}}{\partial x_k\partial x_l}\right)\right] \equiv 0. \tag{B4}$$

Indeed, when changing the order of differentiation in parentheses, the first term on the right-hand side and the difference between the second and third ones change the sign. Thus, the symmetric stress tensor is

$$\begin{aligned}\tilde{\sigma}_{ik} = &-\left(p + \frac{1}{8\pi}H^2\right)\delta_{ik} + \eta\left(\frac{\partial v_i}{\partial x_k} + \frac{\partial v_k}{\partial x_i}\right) + \frac{1}{2}(M_i H_k + M_k H_i)\\ &+ \frac{1}{4\pi}H_i H_k + \frac{\eta'}{2}\frac{\partial}{\partial x_l}\left(\frac{\partial\omega_{kl}}{\partial x_i} + \frac{\partial\omega_{il}}{\partial x_k}\right).\end{aligned} \tag{B5}$$

Let consider what kind of physics is behind of this arithmetic. The total force $\boldsymbol{\mathcal{F}}$ acting on some portion of the fluid represents the volume integral of the force density, $\int \mathbf{F}\, dV$, reducible to an integral over the surface of the portion. This conversion is performed automatically due to *definition* of the stress tensor: $F_i = \partial\sigma_{ik}/\partial x_k$. Hence,

$$\mathcal{F}_i = \int F_i\, dV = \int \partial\sigma_{ik}/\partial x_k\, dV = \oint \sigma_{ik}\, ds_k,$$

where ds_k are the components of the surface element vector $d\mathbf{s}$.

Similarly, the moment of the forces $\boldsymbol{\mathcal{N}} = \int(\mathbf{F}\times\mathbf{r})dV$ applied to a fluid volume can be expressed as an integral over its surface. Substituting the force components via σ_{ik}, we find

$$\mathcal{N}_{ik} = \oint(\sigma_{il}\, x_k - \sigma_{kl}\, x_i)ds_l + \int(\sigma_{ki} - \sigma_{ik})dV. \tag{B6}$$

Here the volume integral vanishes either if σ_{ik} is a symmetric tensor or the difference $\sigma_{ik} - \sigma_{ki}$ reduces to a divergence of a tensor of the rank three antisymmetric in first pair of indices [44]. The latter is just the case under consideration: from (B2),

$$\sigma_{ik} - \sigma_{ki} = \eta'\frac{\partial^2\omega_{ik}}{\partial x_l^2} = \eta'\frac{\partial}{\partial x_l}\omega_{ikl}, \quad \text{where} \quad \omega_{ikl} = -\omega_{kil} \equiv \frac{\partial\omega_{ik}}{\partial x_l}.$$

Finally, we obtain

$$\mathcal{N}_{ik} = \oint \left(\sigma_{il} x_k - \sigma_{kl} x_i - \eta' \frac{\partial \omega_{ik}}{\partial x_l} \right) ds_l = \oint (\tilde{\sigma}_{il} x_k - \tilde{\sigma}_{kl} x_i) ds_l. \tag{B7}$$

Thus, the ferrofluid stress tensor can always be represented in symmetric form (B5). So the frequent separation of some antisymmetric part from $\tilde{\sigma}_{ik}$ is analogous to the representation of an even number as a sum of two odd ones.

[1] M. I. Shliomis and K. I. Morozov, Negative viscosity of ferrofluid under alternating magnetic field, Phys. Fluids **6**, 2855 (1994).

[2] J.-C. Bacri, R. Perzynski, M. I. Shliomis, and G. I. Burde, "Negative Viscosity" Effect in a Magnetic Fluid, Phys. Rev. Lett. **75**, 2128 (1995).

[3] A. Zeuner, R. Richter, and I. Rehberg, Experiments on negative and positive magnetoviscosity in an alternating magnetic field, Phys. Rev. E **58**, 6287 (1998).

[4] F. Gazeau, B. M. Heegaard, J.-C. Bacri, A. Cebers, and R. Perzynski, Magnetic susceptibility in a rotating ferrofluid: Magneto-vortical resonance, Europhys. Lett. **35**, 609 (1996).

[5] F. Gazeau, C. Baravian, J.-C. Bacri, R. Perzynski, and M. I. Shliomis, Energy conversion in ferrofluids: Magnetic nanoparticles as motors or generators, Phys. Rev. E **56**, 614 (1997).

[6] R. Moskowitz and R. E. Rosensweig, Nonmechanical torque-driven flow of a ferromagnetic fluid by an electromagnetic field, Appl. Phys. Lett. **11**, 301 (1967).

[7] V. M. Zaitsev and M. I. Shliomis, Entrainment of ferromagnetic suspension by a rotating field, J. Appl. Mech. Tech. Phys. **10**, 696 (1969).

[8] Y. I. Frenkel, *Kinetic Theory of Liquids* (Dover, New York, 1955).

[9] D. W. Condiff and J. S. Dahler, Fluid mechanical aspects of antisymmetric stress, Phys. Fluids **7**, 842 (1964).

[10] M. I. Shliomis, Hydrodynamics of a liquid with intrinsic rotation, Zh. Eksp. Teor. Fiz. **51**, 258 (1966) [Sov. Phys. JETP **24**, 173 (1967)].

[11] H. Brenner, Antisymmetric stresses induced by the rigid-body rotation of dipolar suspensions, Int. J. Eng. Sci. **22**, 645 (1984).

[12] B. A. Finlayson, Spin-up of ferrofluids: The impact of the spin viscosity and the Langevin function, Phys. Fluids **25**, 073101 (2013).

[13] R. Brown and T. S. Horsnell, The wrong way round, Electr. Rev. **183**, 235 (1969).

[14] I. Y. Kagan, V. G. Rykov, and E. I. Yantovskii, Flow of a dielectric ferromagnetic suspension in a rotating magnetic field, Magnetohydrodynamics **9**, 258 (1973).

[15] R. E. Rosensweig, J. Popplewell, and R. J. Johnston, Magnetic fluid motion in rotating field, J. Magn. Magn. Mater. **85**, 171 (1990).

[16] A. D. Rosenthal, C. Rinaldi, T. Franklin, and M. Zahn, Torque measurements in spin-up flow of ferrofluids, J. Fluids Eng. **126**, 205 (2004).

[17] A. Chaves, C. Rinaldi, S. Elborai, X. He, and M. Zahn, Bulk Flow in Ferrofluids in a Uniform Rotating Magnetic Field, Phys. Rev. Lett. **96**, 194501 (2006).

[18] A. Chaves, M. Zahn, and C. Rinaldi, Spin-up flow of ferrofluids: Asymptotic theory and experimental measurements, Phys. Fluids **20**, 053102 (2008).

[19] I. Torres-Diaz, A. Cortes, Y. Cedeño-Mattei, O. Perales-Perez, and C. Rinaldi, Flows and torques in Brownian ferrofluids subjected to rotating uniform magnetic fields in a cylindrical and annular geometry, Phys. Fluids **26**, 012004 (2014).

[20] A. V. Lebedev and A. F. Pshenichnikov, Motion of a magnetic fluid in a rotating magnetic field, Magnetohydrodynamics **27**, 4 (1991).

[21] As the result, the stability of the magnetic colloid increases: the dimensionless parameter $m^2/(d_h^3 kT)$ characterizing the interparticle attraction decreases by 8–15 times.

[22] M. I. Shliomis, Magnetic fluids, Usp. Fiz. Nauk **112**, 427 (1974) [Sov. Phys. Usp. **17**, 153 (1974)].
[23] M. I. Shliomis, Effective viscosity of magnetic suspensions, Zh. Eksp. Teor. Fiz. **61**, 2411 (1971) [Sov. Phys. JETP **34**, 1291 (1972)].
[24] K. R. Schumacher, I. Sellien, G. S. Knoke, T. Cader, and B. A. Finlayson, Experiment and simulation of laminar and turbulent ferrofluid pipe flow in an oscillating magnetic field, Phys. Rev. E **67**, 026308 (2003).
[25] R. E. Rosensweig, *Ferrohydrodynamics* (Dover, Mineola, NY, 1997).
[26] S. Feng, A. L. Graham, J. R. Abbott, and H. Brenner, Antisymmetric stresses in suspensions: Vortex viscosity and energy dissipation, J. Fluid Mech. **563**, 97 (2006).
[27] C. Rinaldi and M. Zahn, Effects of spin viscosity on ferrofluid flow profiles in alternating and rotating magnetic fields, Phys. Fluids **14**, 2847 (2002).
[28] M. I. Shliomis, Ferrohydrodynamics: Testing a third magnetization equation, Phys. Rev. E **64**, 060501(R) (2001).
[29] For $\kappa R \gg 1$ the value of $r_m = R[1 - \ln(\kappa R)/(\kappa R)]$ satisfies the equation $I_n(\kappa r_m)/I_n(\kappa R) = (\kappa R)^{-1}$.
[30] B. A. Finlayson, Modeling a ferrofluid in a rotating magnetic field, in *Proceedings of the Comsol Conference, October, Boston, 2007*; see http://www.comsol.com/papers/3204/; accessed July 3, 2012.
[31] L. D. Landau and E. M. Lifshitz, *Fluid Mechanics*, 2nd ed. (Pergamon, Oxford, 1987).
[32] A. V. Lebedev and A. F. Pshenichnikov, Rotational effect: The influence of free or solid moving boundaries, J. Magn. Magn. Mater. **122**, 227 (1993).
[33] M. I. Shliomis, T. P. Lyubimova, and D. V. Lyubimov, Ferrohydrodynamics: An essay on the progress of ideas, Chem. Eng. Commun. **67**, 275 (1988).
[34] A. F. Pshenichnikov, Magnetic fluid motion driven by a high-frequency rotating magnetic field, Fluid Dyn. **31**, 14 (1996).
[35] A. F. Pshenichnikov, A. V. Lebedev, and M. I. Shliomis, On the rotational effect in nonuniform magnetic fluids, Magnetohydrodynamics **36**, 275 (2000).
[36] In experiments [20], the spin-up was observed in a rotating field $H_0 = 46$ Oe. For magnetite particles with a diameter of $d_m = 12$–14 nm such a field corresponds to $\alpha \simeq 0.6$.
[37] G. Z. Gershuni, E. M. Zhukhovitskii, and A. A. Yakimov, On the stability of steady convective motion generated by internal heat sources, J. Appl. Math. Mech. **34**, 669 (1970).
[38] D. J. Bonthuis, D. Horinek, L. Bocquet, and R. R. Netz, Electrohydraulic Power Conversion in Planar Nanochannels, Phys. Rev. Lett. **103**, 144503 (2009).
[39] J. S. Hansen, H. Bruus, B. D. Todd, and P. J. Daivis, Rotational and spin viscosities of water: Application to nanofluidics, J. Chem. Phys. **133**, 144906 (2010).
[40] S. De Luca, B. D. Todd, J. S. Hansen, and P. J. Daivis, Electropumping of water with rotating electric fields, J. Chem. Phys. **138**, 154712 (2013).
[41] B. U. Felderhof, Entrainment by a rotating magnetic field of a ferrofluid contained in a cylinder, Phys. Rev. E **84**, 026312 (2011).
[42] R. Mailfert and A. Martinet, Flow regimes for a magnetic suspension under a rotating magnetic field, J. Phys. **34**, 197 (1973).
[43] M. I. Shliomis, Concerning one gyromagnetic effect in a liquid paramagnet, Zh. Eksp. Teor. Fiz. **66**, 1426 (1974) [Sov. Phys. JETP **39**, 701 (1974)].
[44] P. C. Martin, O. Parodi, and P. S. Pershan, Unified hydrodynamic theory for crystals, liquid crystals, and normal fluids, Phys. Rev. A **6**, 2401 (1972).